Changes in Ca^{2+} Affinity upon Activation of *Agkistrodon piscivorus piscivorus* Phospholipase A_2[†]

Brian Lathrop,[‡] Martha Gadd,[‡] Rodney L. Biltonen,[‡] and Gordon S. Rule*[,§]

Departments of Pharmacology and Biochemistry and Molecular Genetics, University of Virginia School of Medicine, Charlottesville, Virginia 22908, and Department of Biological Sciences, Carnegie Mellon University, 4400 Fifth Avenue, Pittsburgh, Pennsylvania 15213-3890

Received August 11, 2000; Revised Manuscript Received November 14, 2000

ABSTRACT: Changes in the affinity of calcium for phospholipase A_2 from *Agkistrodon piscivorus piscivorus* during activation of the enzyme on the surface of phosphatidylcholine vesicles have been investigated by site-directed mutagenesis and fluorescence spectroscopy. Changes in fluorescence that occur during lipid binding and subsequent activation have been ascribed to each of the three individual Trp residues in the protein. This was accomplished by generating a panel of mutant proteins, each of which lacks one or more Trp residues. Both Trp21, which is found in the interfacial binding region, and Trp119 show changes in fluorescence upon protein binding to small unilamellar zwitterionic vesicles or large unilamellar vesicles containing sufficient anionic lipid. Trp31, which is near the Ca^{2+} binding loop, exhibits little change in fluorescence upon lipid bilayer binding. A change in the fluorescence of the protein also occurs during activation of the enzyme. These changes arise from residue Trp31 as well as residues Trp21 and Trp119. The calcium dependence of the fluorescence change of Trp31 indicates that the affinity of the enzyme for calcium increases at least 3 orders of magnitude upon activation. These studies suggest either that a change in conformation of the enzyme occurs upon activation or that the increase in calcium affinity reflects formation of a ternary complex of calcium, enzyme, and substrate.

Soluble phospholipase A_2 (PLA_2,[1] EC 3.1.1.4) are calcium-dependent lipases, which catalyze the hydrolysis of the *sn*-2 ester linkage from phosphophatidylglycerides (for reviews, see refs *4*−*7*). Phospholipases are active against monomeric and micellar substrates, small unilamellar vesicles (SUV), and large unilamellar vesicles (LUV). However, maximum rates of hydrolysis of aggregated substrates are often many orders of magnitude faster than rates observed for monomeric substrates (*8*). The hydrolysis of SUV (*9*) and anionic phosphomethanol vesicles (*9*) can be approximately modeled with a normal Michaelis−Menten kinetic scheme. However, the hydrolysis of zwitterionic phosphophatidylcholine LUV exhibits complex time courses (*10*−*12*). At temperatures above and below the phase transition, the initial rate of product formation is characterized by an initial phase of very slow hydrolysis (the lag phase) followed by a large increase, or burst, of activity. The dependence of the time of lag phase on the dipalmitoylphosphatidylcholine (DPPC) LUV concentration is biphasic; the lag time initially decreases as the substrate concentration is increased, reaches a minimum value, and then increases at higher lipid concentrations (*13*).

The events that lead to activation of the enzyme on the surface of phosphatidylcholine vesicles are poorly understood. Studies by Burack et al. with PLA_2 from *Agkistrodon piscivorus piscivorus* (AppD49) indicate that lateral compositional phase separation (*14*) and changes in vesicle morphology (*15*) occur when the mole fraction of products exceeds ∼0.08. This phase separation coincides with activation of the enzyme. Fluorescence spectroscopy has shown that conformational changes of this enzyme may occur during activation (*10*). FTIR studies on AppD49 on supported DPPG/DPPC (0.2:0.8) bilayers show that amide exchange is significantly faster for the bound enzyme than the enzyme in solution (*16*). Computer modeling (*17*, *18*) of the time course of hydrolysis of DPPC LUV suggests that activation of the enzyme may be due to the formation of increasing concentrations of an active form of the enzyme on the vesicle surface as product accumulates during the lag phase.

The molecular mechanism of increased activity toward aggregated substrates is currently unknown. The initial binding of phospholipases to aggregated substrates occurs via an interfacial region on the protein that surrounds the active site region. The most compelling evidence for the

[†] This work was supported by a grant from the NSF (DMB9305002) to G.S.R. and R.L.B. and by a grant from the NIH (GM37658) to R.L.B. The NMR spectrometer was purchased, in part, by a shared equipment grant from the NSF (BIR-9217013). Equipment for protein purification was obtained, in part, through a shared equipment grant from the NSF (BIR-9216996).

* To whom correspondence and reprint requests should be addressed.
[‡] University of Virginia School of Medicine.
[§] Carnegie Mellon University.

[1] Abbreviations: AppD49, monomeric phospholipase A_2 from the venom of *A. piscivorus piscivorus*; $rPLA_2$, recombinant form of AppD49; $W31^+$, form of $rPLA_2$ containing the W21F and W119Y mutations; DHPC, dihexadecylphosphatidylcholine; diC4 PC, dibutylphosphatidylcholine; DPPC, dipalmitoylphosphatidylcholine; SUV, small unilamellar vesicles; LUV, large unilamellar vesicles; MLV, multilamellar vesicles; EGTA, ethylene glycol bis(β-aminoethyl ether)-*N*,*N*,*N*′,*N*′-tetraacetic acid; HSQC, heteronuclear single-quantum correlation.

10.1021/bi001901n CCC: $20.00
Published on Web 02/20/2001

existence of a well-defined interfacial region was provided by electron spin resonance relaxation measurements that determined the orientation of bee venom lipase on the membrane surface (*19*). The binding of lipases to vesicle surfaces appears to utilize both electrostatic forces and hydrophobic and hydrogen bonding interactions (see ref *20* for a review). For lipases that possess high affinity for anionic vesicles, the binding appears to involve the interaction between positively charged lysine residues and the negative charge of the lipid. Mutagenesis studies by Han et al. (*21*) on AppD49 suggest that Lys7, Lys10, Lys11, and, to a lesser extent, Lys16 play a significant role in the binding of AppD49 to anionic lipids.[2] In contrast, the lipase from bee venom does not appear to utilize electrostatic interactions to bind to anionic vesicles (*22*). Lipases that show high affinity for neutral vesicles appear to utilize aromatic residues in the interfacial region to bind to the vesicle surface. Cho and co-workers have shown that Tyr3, Trp19, Trp61, Phe64, and Tyr110 play an important role in the binding of the phospholipase from *Naja naja atra* to zwitterionic vesicles (*23*).

NMR studies on PLA_2 from porcine pancreas (*24*) have suggested that stabilization of the amino-terminal helix is an important step in activation of the bound enzyme on aggregated surfaces. This stabilization may affect the structure of the catalytic site by permitting the formation of a hydrogen-bonded network that extends from the amino terminus to the active site (*24*). It is not clear how significant the formation of the amino-terminal helix is in enhancing catalytic activity because deletion of the amino-terminal residue does not affect k_{cat} (*25*). Furthermore, NMR studies show that this helix is well formed in solution for AppD49 (*26*). Thus, the changes in fluorescence and amide exchange noted above are unlikely to be associated directly with stability of this helix.

Other structural changes in the active site region may occur during activation. Lathrop and Biltonen (*9*) have previously shown that, using DPPC SUV as a substrate, the apparent pK_D of Ca^{2+} of AppD49 is ~40 μM compared to ~2 mM for the enzyme in solution. This large difference in affinity for calcium has been largely ignored in discussing the details of the mechanism of activation of PLA_2. Insofar as deduction of this large change in affinity required estimation of the initial velocity following correction for product inhibition, some doubt remains as to size of this estimated change in affinity.

To obtain a better estimate of the change in affinity for Ca^{2+} and any conformational changes that may occur during activation of AppD49, a series of experiments have been initiated to localize the fluorescence changes that occur during activation. The approach has been to selectively replace one or more of the three tryptophan (Trp) residues in AppD49 such that the contribution of each Trp residue to the intrinsic fluorescence of the protein can be gauged. The fluorescent properties of these mutants suggest that the environments of Trp21 and Trp119 are sensitive to enzyme−lipid interactions, while Trp31 is most affected by Ca^{2+} binding. These studies show that the Ca^{2+} affinity for the activated enzyme−bilayer complex is at least 1000-fold higher than the affinity in solution.

[2] The residue numbering system that is used is based on the homologous core developed by Renetseder et al. (*1*) and the corrected sequence of Maraganore and Heinrikson (*2, 3*).

MATERIALS AND METHODS

Preparation of Enzymes. Venom of *A. piscivorus piscivorus* was obtained from Sigma Chemical Co. The basic, monomeric, Asp49 isozyme of phospholipase A_2 was purified from venom according to published procedures (*27*). The resulting purified enzyme, AppD49, was dissolved in 50 mM KCl. The enzyme concentration was determined from its absorption at 280 nm using an $\epsilon_{280,1\%}$ of 22.0. The recombinant enzyme ($rPLA_2$) was obtained by expression of a synthetic gene for AppD49 in *Escherichia coli*. The amino acid sequence of the recombinant protein differs from that of the venom enzyme by substitution of the amino-terminal Asn in $vPLA_2$ with Ser in $rPLA_2$. This change was required to enhance the removal of the initiator Met residue by bacterial methionine aminopeptidase (*28*). Pure $rPLA_2$ was obtained from bacterial inclusion bodies by refolding and reoxidation of the sulfonated protein (see ref *26* for additional details).

The gene for N-Ser PLA_2 was cloned into M13mp18 (*29*) and used as a template for site-directed mutation using the Kunkel method (*30*). Trp21 and -31 were converted to Phe, while Trp119 was converted to Tyr. The $W31^+$ mutant (W21F and W119Y) was constructed by subcloning various fragments from mutant and wild-type genes. The sequence of all mutant genes was confirmed by double-stranded sequencing using the chain termination method (*31*). Purification of the mutant proteins was accomplished using the same scheme as for $rPLA_2$. However, the yields of W31F were low, precluding a detailed kinetic analysis of this mutant.

Preparation of Lipid Vesicles. DPPC and diC4 PC were purchased from Avanti Polar Lipids (Alabaster, AL). DHPC was purchased from Fluka Biochemicals (Ronkonkoma, NY). All lipids were used without further purification. MLV were prepared as previously described (*9*). SUV were prepared from MLV by sonication above the gel−fluid transition temperature. DPPC LUV were prepared from MLV by extrusion as described previously (*13*). Extruded LUV were equilibrated with the appropriate buffer by heating and cooling through the phase transition region (T_m = 41 °C) five times prior to being used. LUV were stored at 45 °C on the day of use. The monomeric substrate, diC4 PC, was dried from chloroform, lyophilized, and resuspended to a concentration of ~100 mM in 50 mM KCl. This stock solution was diluted to 5 mM for enzyme assays, well below its CMC of 250−280 mM. The concentrations of all lipid stocks were determined as previously described (*9*).

Determination of Enzyme Activity. The hydrolysis of monomeric diC4 PC and DPPC SUV was followed by measuring the moles of base required to maintain the pH at 8 using a pH stat in the autotitration mode. The apparent K_m and k_{cat} were determined by examination of hydrolysis of DPPC SUV (enzyme concentration = 7 nM, Ca^{2+} concentration = 10 mM, T = 23 °C) as a function of substrate concentration. To perform steady state measurements, product inhibition was alleviated by including 10 mM Mg^{2+} in the reaction buffer (*9*). The dependence of the initial velocity, V_o, on the substrate concentration, [S], was fit to eq 1:

$$V_o = k_{cat}[E][S]/(K_m + [S]) \quad (1)$$

where k_{cat} is the apparent turnover number and K_m is the Michealis−Menten constant.

DPPC LUV enzyme assays were, on occasion, performed simultaneously with measurements of Trp fluorescence by placing the buret tip and combination electrode of the pH stat directly into the cuvette of the fluorometer as described previously (*10*). Data from the hydrolysis of LUV were not corrected for product inhibition (*9*) because hydrolysis during the lag phase produces only a small amount of product. The extent of product inhibition is reduced further by the fact that the slow hydrolysis rate permits diffusion of the products away from the enzyme.

Fluorescence Studies. The dissociation constant, K_d, for Ca^{2+} was determined by measuring the Ca^{2+}-dependent change in the intrinsic fluorescence of the protein. Measurements were made with a SLM8000C spectrofluorometer; additional details can be found in ref *9*. The K_d for gel state DPPC SUV was determined by quantifying the lipid-dependent change in the intrinsic fluorescence of the protein (300 nM) in the absence of Ca^{2+}. EGTA (10 mM) was added to inhibit phospholipid hydrolysis. The excitation wavelength was 280 nm, and the emission wavelength was 340 nm. Light scattering from SUV was assessed independently and subtracted from the emission intensity. The K_d values were determined by fitting the measured change in fluorescence relative to the fluorescence in the absence of lipid, ΔF, to eq 2. ΔF_{max} is the relative change in fluorescence at saturating [S].

$$\Delta F = \Delta F_{max}[S]/(K_d + [S]) \quad (2)$$

Changes in protein fluorescence during hydrolysis were monitored coincidentally with pH changes during the reaction as described above. The calcium dependence of the fluorescence change of $W31^+$ during the burst phase was obtained by adding sufficient Ca^{2+} above the concentration of EGTA to obtain the desired free Ca^{2+} concentration. Lag times at Ca^{2+} concentrations of less than 3 μM were not very reproducible. This is in part due to difficulty in accurately assessing the Ca^{2+} concentration.

NMR Spectra. All spectra were acquired on a Varian UnityPlus 500 MHz NMR spectrometer at 40 °C. The samples contained 100 μM protein, in 20 mM sodium phosphate (pH 4.6) and 100 mM KCl. Spectra were acquired with a sweep width of 8 kHz (16K complex points) using a relaxation delay of 1 s. The total acquisition time was 20 min. Data were processed using Felix98 (Molecular Simulations Inc.) using a 1 Hz line broadening function. $^1H-^{15}N$ heteronuclear correlated spectra (HSQC) were acquired as previously described (*26*).

RESULTS

Calcium Dependence of the Time Course of AppD49 Hydrolysis of DPPC LUV. The time course of hydrolysis of DPPC LUV by $vPLA_2$ is characterized by a lag phase followed by a sudden burst in activity. The time of the burst can be accurately estimated by monitoring the amount of base used to neutralize the fatty acid product, the change in the intrinsic fluorescence of the protein, changes in a fluorescence probe such as a pyrene-labeled fatty acid, or changes in the amount of light scattered by the vesicles. Time courses at three different Ca^{2+} concentrations, obtained using the pH stat method, are shown in Figure 1. The lag time, τ, is shown as a function of Ca^{2+} concentration in Figure 2A. The same data, represented as $1/\tau$ versus $\log[Ca^{2+}]$ in Figure 2B, have been fit to eq 3.

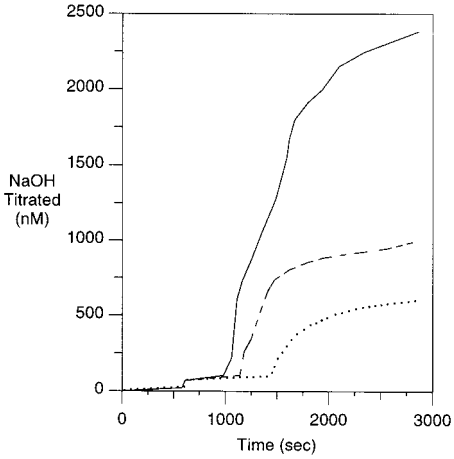

FIGURE 1: Effect of calcium on τ for DPPC LUV. The reaction was initiated by the addition of 300 nM AppD49 at 550 s. The excess calcium was 1 mM (—), 100 μM (− − −), and 10 μM (•••). Other conditions were 1 mM DPPC, 50 mM KCl, 10 μM NaN_3, 10 μM EGTA, 38.5 °C.

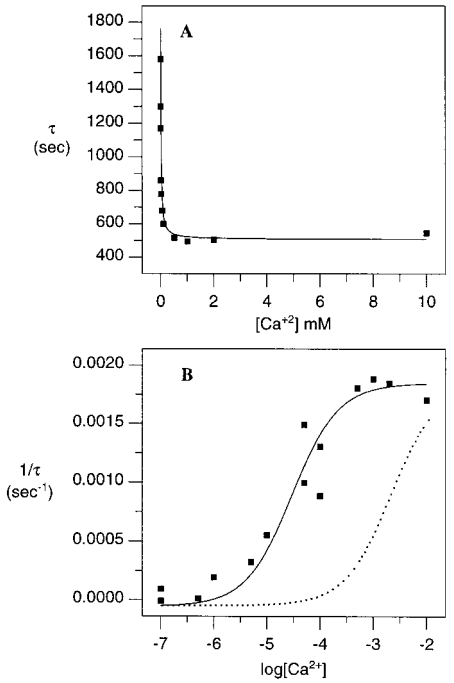

FIGURE 2: Summary of the effect of calcium on τ as monitored by pH titration. τ is plotted as a function of $[Ca^{2+}]$ in panel A. The inverse of τ as a function of $\log[Ca^{2+}]$ is plotted in panel B. In both panels, the solid line is generated from a least-squares fit to eq 3 with a K_{app} value of 30 μM. The dotted line in panel B was calculated assuming a K_{app} value of 2 mM. The conditions of the experiments were as described in the legend of Figure 1.

$$1/\tau = A[Ca^{2+}]/(K_{app} + [Ca^{2+}]) \quad (3)$$

where A is the limiting value of $1/\tau$ at infinite $[Ca^{2+}]$ and K_{app} is a phenomenological dissociation constant for Ca^{2+}.

The solid line is calculated for an A of 0.0018 s^{-1}, and K_{app} is 30 μM. The dotted line was calculated assuming the

Table 1: Thermodynamic and Kinetic Properties of *A. piscivorous piscivorous* Phospholipase A_2 and Its Tryptophan Mutants

	AppD49[a]	$rPLA_2$	Trp21F	Trp31F	Trp119Y	W31+ [b]
monomer kinetics[c]						
V_o (diC4 PC)	1.0 ± 0.1	1.0	1.0	1.0	0.6	0.5
SUV kinetics[d]						
K_m (mM)	0.14 ± 0.04	0.36	0.10	ND[e]	0.4	0.5
k_{cat} (s^{-1})	350 ± 20	310	300	ND[e]	428	300
DPPC SUV binding[d]						
K_d (mM)	0.06 ± 0.006	0.11	0.28	0.49	0.41	0.31
$n\Delta F_{max}$[f]	2.8	2.6	1.6	2.5	2.2	0.5
Ca^{2+} binding						
$K_{d\,(mM)}$	2.6 ± 0.1	2.8	1.9	ND[g]	2.1	1.8
$n\Delta F_{max}$[f]	1.1	1.2	1.1	ND[g]	1.0	1.1

[a] The relative errors listed for the wild-type enzyme apply to all other species as well. [b] $W31^+$ is the W21F/W119Y double mutant. [c] Activity expressed relative to venom PLA_2 (WT) = 1.0. The activity of this enzyme is ~4 s^{-1} toward 5 mM micelles and 10 mM $CaC1_2$ (pH 8.0). [d] SUV refers to DPPC small unilamellar vesicles. All experiments were carried out at 25 °C and pH 8.0. Binding was assessed in the presence of 10 mM EGTA. Hydrolysis was assessed in 10 mM $CaC1_2$. Other details are given in Materials and Methods. [e] Not determined. [f] ΔF_{max} is the relative change in fluorescence extrapolated to saturating conditions. [g] Not determined. No fluorescence change detected and K_d could not be determined.

same value for A and assuming $K_{app} = 2$ mM, the dissociation constant for the free enzyme. It has previously been shown that τ is the time required to hydrolyze a constant mole fraction of substrate. It therefore follows that $1/\tau$ is proportional to a rate constant times the amount of active enzyme. Interpretation of these results in terms of the model described by eq 3 is that an "active" form of the enzyme exists during the lag phase, it requires Ca^{2+}, and its interaction with the cation is described by an apparent dissociation constant of 30 μM. This interpretation is consistent with the results of Lathrop and Biltonen (*9*) using DPPC SUV as a substrate. However, it can be shown with straightforward thermodynamics arguments that $K_{app} = K_d/f_o$, where f_o is the fraction of active enzyme in the absence of Ca^{2+} and K_d is the intrinsic dissociation constant of the active form. It is thus possible that the small amount of hydrolysis occurring during the lag phase is the result of a small amount of the active form with a K_d that is significantly less that 30 μM.

It must be emphasized that the above analysis is only applicable to the state of the enzyme during the lag phase, and the question still remains as to its relationship to the events occurring at the burst in activity. To seek answers to these questions, a series of tryptophan mutants were engineered to characterize structural changes in the enzyme due to lipid binding and activation.

Characterization of Mutant Proteins. The three Trp residues in $rPLA_2$ were altered by site-directed mutagenesis. Four enzymes with altered Trp residues have been characterized. Three of these engineered proteins have single-amino acid changes (W21F, W31F, and W119Y), and one has two changes (W21F and W119Y). The latter mutant will be termed $W31^+$. The enzymatic properties of all four altered proteins, and AppD49, are similar to those of the native enzyme (see Table 1). The activities of W21F and W31F toward the monomeric substrate diC4 PC are quantitatively similar to those found for AppD49 and $rPLA_2$. The activities of W119Y and $W31^+$ toward the monomeric substrate diC4 PC are 50−60% of that of the native protein. The decrease in activity of the $W31^+$ enzyme can be accounted for solely by the presence of the W119Y mutation. It therefore appears that the two alterations in the $W31^+$ enzyme have no greater effect on the activity toward the monomeric substrate than either mutation individually. Although the kinetic measurements utilizing monomeric substrate will include a contribution from enzyme absorbed to the surface of the reaction vessel (*32*), it is clear that all of the altered proteins have similar catalytic activities toward the monomeric substrate as the native enzyme.

The activity of $rPLA_2$ and the mutant proteins toward DPPC SUV shows some interesting trends. The K_m of $rPLA_2$ is 2-fold higher than the value found for $vPLA_2$. It has been observed with the pancreatic PLA_2 that alterations of the amino terminus affect binding to phosphatidylcholine vesicles (*25*). Further, note that in the W21F mutant the K_m is similar to that found for vPLA $_2$. Position 21 is close to the interfacial binding region (*19*, *33*), and alterations at this position appear to compensate for the amino-terminal alteration of Asn to Ser. Three proteins ($rPLA_2$, W21F, and $W31^+$) have identical k_{cat} values, which suggest that the catalytic mechanism is not affected by these. Kinetic parameters for W31F toward DPPC SUV were not obtained because of the limited yields of this protein.

Although the above results show that the altered proteins have enzymatic properties similar to those of the wild-type enzyme, it is important to show that they assume a tertiary structure in solution that is similar to that of the wild-type enzyme. One-dimensional ^1H NMR spectra of AppD49, $rPLA_2$, W21F, W119F, and $W31^+$ show that the aromatic region of the spectrum of these mutant proteins is similar to that of $rPLA_2$, supporting the fact that the structure of these mutant proteins is similar to that of the native protein (data not shown). Therefore, on the basis of the enzymatic data as well as the NMR data, the structures of the Trp mutants appear to be sufficiently similar to that of $rPLA_2$ so that comparisons between these proteins will be meaningful.

Effect of Lipid Binding on the Fluorescence of the Trp Residues in PLA_2. The effect of lipid binding on the environment of each Trp residue in PLA_2 can be determined by an analysis of the changes in fluorescence of the mutated proteins that arise as a result of lipid binding (see Table 1). ΔF_{max} is defined as the experimentally estimated change in fluorescence in the limit of saturating lipid relative to the instrinsic fluourescence of the protein in the absence of lipid. To simplify the analysis, we assumed that the average intrinsic fluorescence of each Trp residue in all species is the same and equal to $F°$. This approximation is valid since the intrinsic fluorescence of each protein is proportional, within 10%, to the number of Trp residues in the protein.

Equation 4 describes the contribution of each Trp residue to the overall fluorescence.

$$\Delta F_{max} = \sum \alpha_j \Delta F_{j,max}/nF^\circ \quad (4)$$

$\alpha_j = 1$ or 0 depending on whether a specific residue is a Trp or not. $\Delta F_{j,max}$ is the maximal change in fluorescence in residue *j*, and *n* is the number of Trp residues of a particular protein species.

We find that if both Trp21 and Trp119 are present (AppD49 and rPLA$_2$) then $n\Delta F_{max} = 2.7 \pm 0.1$. However, if both Trp21 and Trp119 are mutated (W31$^+$), then $\Delta F_{max} = 0.5$. Solving the six simultaneous equations generated by six enzyme species yields best estimates of $\Delta F_{j,max}/F^\circ$ of 1.4 $\pm$ 0.1 for Trp21, 0.9 $\pm$ 0.1 for Trp119, and 0.0 $\pm$ 0.1 for Trp31. Thus, the fluorescence change observed upon lipid binding is dominated by Trp21 and Trp119. On the basis of this analysis, Trp31 contributes less than 10% to the lipid-induced changes in fluorescence. The small lipid-induced fluorescence change observed for W31$^+$ (see Table 1) may be a consequence of the two altered Trp residues in this protein. The small contribution of Trp31 to the lipid-induced fluorescence changes is consistent with the fluorescence quenching studies of Yu et al. which showed that residue 31 in the pancreatic enzyme is fully exposed to solvent in the presence of membrane vesicles (*34*).

The dissociation constants for the interaction of AppD49 and rPLA$_2$ with DPPC SUV were in reasonable agreement (Table 1). However, K_d increases by factors of 3−5 for the various Trp mutants. This amounts to ~0.6−1.0 kcal/mol in the change in the Gibbs energy. This change is either due to changes in specific interactions between the lipid bilayer and the Trp residues or due to subtle changes in the protein due to the mutation.

Effect of Ca^{2+} Binding on the Fluorescence of the Trp Residues in PLA$_2$. Changes in protein fluorescence can be used to monitor Ca^{2+} binding to AppD49 and several of the mutant species (Figure 3). The results are summarized in Table 1. In all cases where a fluorescence change was observed, K_d was in the range of 2.3 $\pm$ 0.5 mM. However, the magnitude of the fluorescence changes was extremely sensitive to the enzyme species being investigated. The fact that the $n\Delta F_{max}$ values are all equal to 1.1 $\pm$ 0.1 indicates that a single residue is contributing to the calcium-induced fluorescence. Solving the simultaneous equations given by eq 4 provides best estimates for $\Delta F_{j,max}/F^\circ$ of 1.1 $\pm$ 0.1 for Trp31 and 0.0 $\pm$ 0.1 for Trp21 and Trp119. It thus appears that only Trp31 contributes to the fluorescence change resulting from calcium binding. This is underscored by the fact that W31F, which is missing only Trp31, does not exhibit a change in fluorescence in the presence of calcium ion.

The contribution of Trp31 to calcium-induced changes in fluorescence is not surprising since the peptide carbonyl oxygens of residues 28, 30, and 32 are part of the specific calcium binding loop, defining an isosceles triangle in which Ca^{2+} is located (*21*, *35*). The observed changes in the environment of Trp31 are also consistent with the work of Kuipers et al (*36*), who demonstrated that calcium has a strong influence on the excited state population distribution in a mutant of porcine pancreas PLA$_2$ containing a single Trp at position 31. Furthermore, NMR studies (*26*) indicate that residues in the region of the Ca^{2+} binding loop show

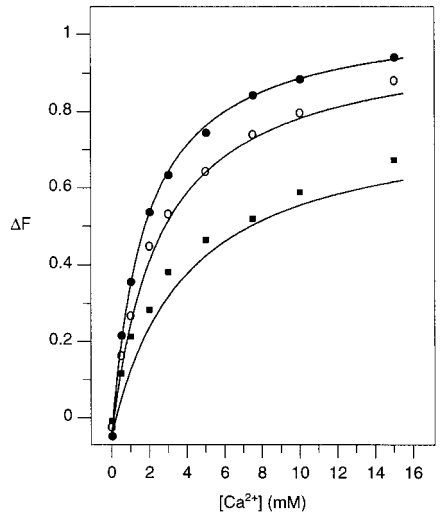

FIGURE 3: Ca^{2+} binding to AppD49 and W31$^+$. The dependence of enzyme fluorescence on [Ca^{2+}] is shown for AppD49 (○) and W31$^+$ (●) in solution and for W31$^+$ bound to SUVs of dihexadecylphosphatidylcholine (■). The enzyme concentration was 300 nM, and the experiment was performed in the presence of 10 mM EGTA. The excitation wavelength was 280 nm, and emission was monitored at 340 nm. Light scattering was measured separately and subtracted from the emission intensity. The data were analyzed according to eq 2.

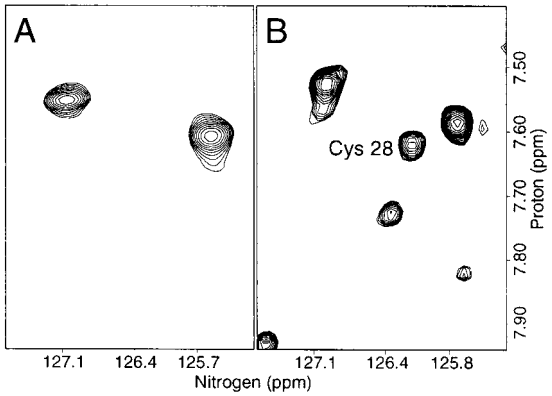

FIGURE 4: ^{1}H−^{15}N HSQC spectra of rPLA$_2$. A small region of the HSQC spectra of ^{15}N-labeled rPLA$_2$ in the absence (A) and presence of Ca^{2+} (B). The peak assigned to Cys28 cannot be found in the spectra acquired in the absence of Ca^{2+}.

dynamic behavior in the absence of Ca^{2+} because their amide resonance lines are either broad or missing (e.g., residue Cys28) from the ^{1}H−^{15}N correlated spectrum of the calcium free enzyme. Addition of Ca^{2+} to the enzyme reduces the degree of exchange broadening for Cys28 (see Figure 4).

Changes in Ca^{2+} Affinity during Activation. Since the fluorescent properties of Trp31 are altered by Ca^{2+} binding, but those of Trp21 and Trp119 are not, W31$^+$ can be used as a sensitive probe to monitor Ca^{2+} binding to the enzyme. The affinity of binding of Ca^{2+} to PLA$_2$ in solution has been determined with fluorescence spectroscopy (Table 1 and Figure 3). In all cases, the K_d for Ca^{2+} was found to be in the range of 1.8−2.6 mM. Therefore, the alterations of residues Trp21, Trp119, and Trp31 do not appear to have significantly affected Ca^{2+} binding to the enzyme in solution. Furthermore, a K_d of 3.9 mM was determined for Ca^{2+} to W31$^+$ bound to the surface of the nonhydrolyzable substrate DHPC SUV (Figure 3). This result is consistent with the conclusion of Bell and Biltonen (*10*), who showed that the

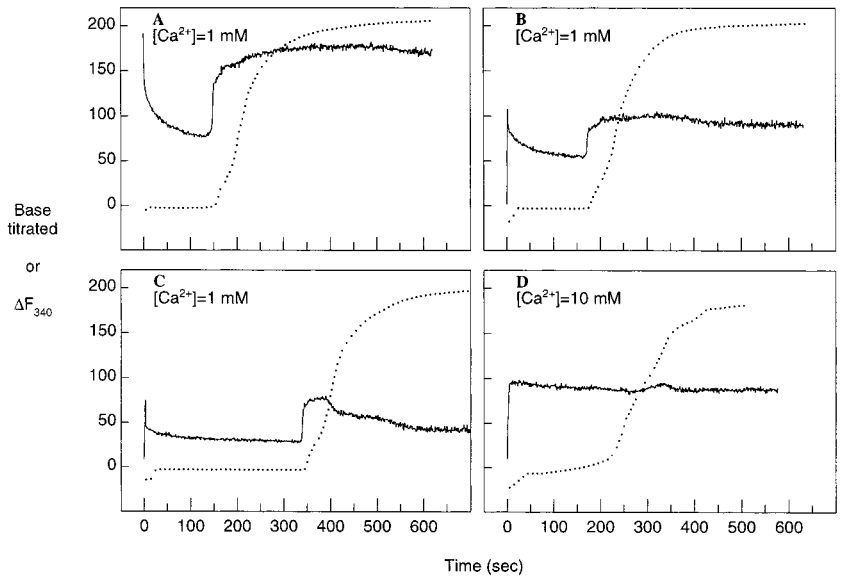

FIGURE 5: Simultaneous changes in enzyme fluorescence and proton release occurring during rapid hydrolysis of DPPC LUV. The time dependence of hydrolysis of DPPC LUVs is shown for AppD49 (A), W31F (B), and $W31^+$ (C and D). Hydrolysis was quantified by the amount of base titrated with a pH stat to maintain the pH at 8.0 (···). The scale on the ordinate refers to nanomolar NaOH added. Enzyme fluorescence was measured simultaneously in the same sample using an SLM 8000 fluorimeter (—). The scale used for the fluorescence changes is not indicated, but was the same in all panels. The excitation wavelength was 280 nm, and the emission wavelength was 340 nm. The concentration of enzyme was 250 nM, and the concentration of DPPC was 100 μM. Measurements were performed at 40 °C in the presence of 1 (A−C) or 10 mM (D) calcium.

affinity of AppD49 for DHPC SUV was not significantly influenced by Ca^{2+}. Since AppD49 binds DPPC and DHPC SUV with approximately equal affinity, it would appear that the K_d values for Ca^{2+} of the solution enzyme and the bilayer-bound enzyme are also essentially identical.

Lathrop and Biltonen (*9*) estimated from catalytic experiments that the apparent K_d of Ca^{2+} for AppD49 under conditions of maximal rate of hydrolysis of SUV was ~40 μM. This value is at least 20-fold smaller than the equilibrium K_d. The latter study was based on measurements of the initial velocity of the hydrolysis reaction as a function of calcium concentration. Although excess Mg^{2+} was included in the reaction mixture to reduce the level of product inhibition, it was still necessary to correct for time-dependent product inhibition, which introduced systematic errors into the analysis. Such a correction is not necessary here because of the slow rate of hydrolysis of LUV. The availability of the $W31^+$ mutant and the use of LUV now allows another approach to determining the apparent K_d for Ca^{2+} binding to the enzyme during catalysis.

Figure 5 shows simultaneous changes in both enzyme fluorescence and product release during PLA_2-catalyzed hydrolysis of DPPC LUV. Panel A shows typical data obtained with AppD49 at 1 mM Ca^{2+}, where only about 30−40% of the enzyme in solution binds Ca^{2+}. After a lag period, the enzyme activity rapidly increases. Concomitantly, there is a large change in protein fluorescence. This change in protein fluorescence arises from changes in the environments of all three Trp residues because fluorescence changes are observed with the Trp31 mutant (panel B) as well as in $W31^+$ (W21F/W119Y; panel C). The observed changes in fluorescence could be a due to several factors: enhanced binding to the bilayer, enhanced Ca^{2+} binding, or a protein conformational change. Panel C should be compared to panel D, where it is shown that in the presence of 10 mM Ca^{2+} $W31^+$ exhibits no significant fluorescence change at the burst.

The change in the fluorescent properties of $W31^+$ during activation could be either due to a change in the occupancy of the Ca^{2+} binding site or due to changes in the intrinsic environment of the fluorophore at activation. These two possibilities can be distinguished by determining the change of $W31^+$ fluorescence as a function of Ca^{2+} concentration. If the fluorescence is the result of changes in the amount of bound calcium, then the magnitude of the fluorescence change should reflect the difference in the degree of site occupancy before and after activation. Figure 5 (panel D) shows that at 10 mM Ca^{2+}, well above the K_d of the solution form of $W31^+$, there is no change in fluorescence from residue W31 because the enzyme is essentially saturated with Ca^{2+} at all times. At lower Ca^{2+} concentrations, when the enzyme is not fully saturated with calcium, a fluorescence change is observed at the beginning of activation. This is consistent with the second hypothesis: the fluorescence change results from an increase in the Ca^{2+} occupancy at the burst.

Fluorescence time courses at different Ca^{2+} concentrations were obtained for $W31^+$ as shown in panels C and D of Figure 5. The reciprocal of the lag time, τ^{-1}, is shown as a function of log[Ca^{2+}] in Figure 6. The same data were fit with eq 3 as described previously. The apparent dissociation constant was estimated to be 80 μM, shown as the solid line. The dotted line was calculated assuming the same value for A used for the analysis of similar data for AppD49 shown in Figure 2 and assuming $K = 1.9$ mM, the dissociation constant for the free enzyme. As with the studies on AppD49, this model suggests that an "active" form of $W31^+$ exists during the lag phase, it requires Ca^{2+}, and its interaction with the cation is described by an apparent dissociation constant of 80 μM.

Activation results in a change in calcium affinity. Therefore, the magnitude of the fluorescence changes that are

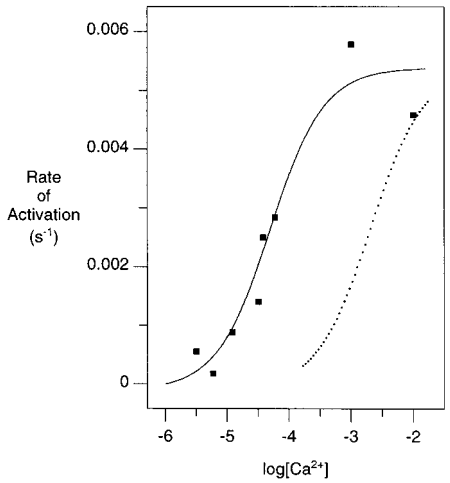

FIGURE 6: Reciprocal of τ for $W31^+$ as a function of log[Ca^{2+}]. The conditions were the same as for the data depicted in Figure 5. These results were analyzed as described in the legend of Figure 2. The solid line was calculated using eq 3 with a K_{app} of 80 μM. The broken line was calculated assuming a K_{app} of 1.9 mM, the value obtained for the enzyme in solution (see Table 1).

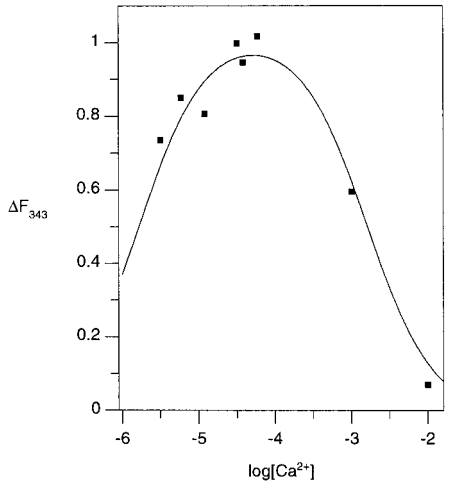

FIGURE 7: Calcium dependence of the change in $W31^+$ fluorescence at the burst as a function of calcium. The relative change in fluorescence of $W31^+$ at the burst, normalized to the maxium change observed, is shown as a function of log[Ca^{2+}]. The data were analyzed according to eq 5, assuming a K_d value of 1.6 mM for the inactive form of the enzyme (see Table 1) and a value of 1.3 μM for the active enzyme.

observed at different calcium concentrations (shown in Figure 7) can be described quantitatively in terms of the dissociation constants for calcium of the active and inactive forms of the enzyme, as shown by eq 5.

$$\Delta F = \Delta F_{max}\Delta Ca^{2+} = \Delta F_{max}[Ca^{2+}][1/(K_d^* + [Ca^{2+}]) - 1/(K_d + [Ca^{2+}])] \quad (5)$$

ΔCa^{2+} is the difference in the degree of saturation between the activated enzyme and the inactive enzyme with dissociation constants K_d^* and K_d, respectively. The other parameters have been defined previously.

The relative changes in fluorescence at the burst were fit to eq 5, and the fitted line is shown in Figure 7. In this analysis, K_d was assumed to be the value obtained for the protein in solution. Analysis of these data yielded an estimate

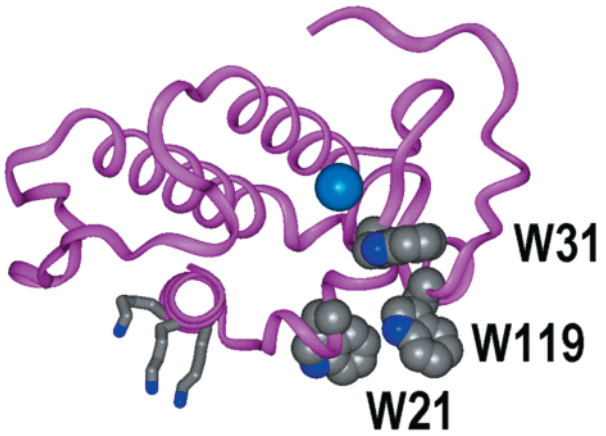

FIGURE 8: Interfacial binding region of AppD49. The structure of AppD49 is shown [1VAP (*21*)]. The protein is oriented such that the plane of the membrane is perpendicular to the page and below the molecule. The peptide chain is rendered as a ribbon. The bound Ca^{2+} ion is the light blue sphere. Lysine residues (K7, K10, and K11) that are responsible for binding to anionic vesicles are rendered in sticks and colored in CPK. The three Trp residues are rendered as space-filling molecules, colored cpk, and labeled. In this orientation, Trp21 and Trp119 are at the base of the molecule and point toward the membrane while Trp31 is located near the center of the protein, close to the bound Ca^{2+} ion. The location of the Ca^{2+} ion was modeled using the structure of the *N. naja atra* enzyme [1POB (*33*)].

of K_d^* of less than 3 μM, almost 1000-fold lower than that observed for the free enzyme. At a Ca^{2+} concentration of 60 μM, the maximum change in fluorescence is observed. At this concentration, the inactive enzyme binds insignificant levels of Ca^{2+}, but upon activation, the enzyme binds near-saturating amounts of Ca^{2+}.

DISCUSSION

As with studies on porcine PLA_2 (*36*) and other membrane proteins (*37*), the deletion of Trp residues at selected locations in the protein has proven to be very useful in deconvoluting spectroscopic signals. The fluorescence change that occurs upon binding of AppD49 to DPPC LUV appears to emulate primarily from residues Trp21 and Trp119. This conclusion is based on the fact that the $W31^+$ mutant shows a relatively small change in fluorescence upon binding to SUV while both W21F and W119Y proteins exhibit substantially larger changes in relative fluorescence. The region of phospholipases that interacts with the lipid surface has been inferred from electron spin resonance studies (*19*) and crystallographic (*2*, *21*), fluorescence (*36*, *38*, *39*), and biochemical studies (*40*, *41*) of several small, secreted PLA_2 enzymes. This region includes an extensive segment of the amino-terminal α-helix (*21*) as well as hydrophobic residues in the vicinity of the active site (*23*). The studies presented here support the involvement of Trp21 and Trp119 in lipid binding. This result is consistent with the work of Dua et al. (*41*), who showed that Lys119 is involved in the binding of porcine pancreatic PLA_2 to bilayer surfaces, and that of Sumandea et al. (*23*), who showed that Tyr119 is involved in the binding of *N. naja atra* to neutral vesicles.

Prior to this study, there has been no direct evidence showing that the region of AppD49 in the vicinity of residues 21 and 119 was involved with binding to the bilayer surface. Figure 8 shows a molecular model of AppD49, indicating

the location of the three Trp residues in AppD49, the location of the catalytic Ca^{2+} ion, and the three Lys residues that are important for binding to anionic vesicles (*21*). As evident from this structure, Trp21 and Trp119 are close to the N-terminal interfacial binding region and thus could participate in lipid binding. Since the binding properties of the mutant proteins are similar to those of the wild-type enzyme, the specific contribution of tryptophan residues at positions 21 and 119 to membrane binding must be small. However, the presence of a hydrophobic residue at these positions may play a significant role in binding to the membrane.

During the hydrolysis of DPPC LUV by AppD49, there is a large change in Trp fluorescence that occurs simultaneously with activation of the enzyme (*10*). The data reported here indicate that this change in fluorescence is due to both a perturbation of the environment of Trp21 and Trp119 and a change in the environment of Trp31. The additional changes in the environment of Trp21 and Trp119 may be associated with changes in the physical properties of the bilayer, which occur as a result of product accumulation that leads to changes in the morphology of the bilayer and subsequent activation of the enzyme. Therefore, these changes in fluorescence either could be due to a change in the interaction of the indole ring with the bilayer or may reflect changes in protein structure upon activation.

The most significant result of the studies presented here is the discovery of a large increase in Ca^{2+} affinity that occurs during the activation step. Previous studies by Lathrop and Biltonen (*9*) indicated that the apparent K_m for Ca^{2+} is in the range of 40 μM during hydrolysis of DPPC SUV by $vPLA_2$. Analysis of our results on the calcium dependence of the lag times in terms of eq 3 with a single apparent dissociation constant of 30 μM is consistent with that estimate. However, this estimate of the dissociation constant must be regarded as an upper estimate of the actual value for the K_d of the activated enzyme, since quantitative interpretation of the data is model-dependent. For example, the results could be equally well represented by a model assuming very low activity associated with an "inactive" enzyme ($K_d = 2$ mM) and an active enzyme with a very low K_d (<10 μM). This latter interpretation is consistent with analysis of the Ca^{2+} dependence of the magnitude of the fluorescence change at the burst for $W31^+$, which leads to an estimate for K_d of ~ 3 μM for the active enzyme. This is a more reliable interpretation of the data because changes in the fluorescence of Trp31 reflect only the change in calcium binding at the burst (i.e., for the active enzyme). In any case, it is clear that the affinity of calcium for PLA_2 increases by at least 2, if not 3, orders of magnitude at the point of maximum activity. It therefore follows that under these conditions the free energy change associated with binding the active enzyme to the bilayer improves by more than 4 kcal/mol of protein in the presence of excess calcium.

The dissociation constant for Ca^{2+} binding to porcine PLA_2 is reported to be 0.28 mM for the enzyme in solution and 0.11 mM for the enzyme in complex with micelles of 1,2-ditetradecyl-*sn*-glycero-3-phosphomethanol (*42*). NMR studies on the complex between porcine PLA_2 and dodecylphosphatidylcholine clearly show differences in the structure of the Ca^{2+} binding loop in the free and bilayer-bound enzyme. These differences presumably can account for the 3-fold difference in the dissociation constant for the two forms of the enzyme. However, the affinity of the bilayer-bound porcine enzyme for Ca^{2+} is still substantially lower than the micromolar dissociation constant found for the activated enzyme in this study. It therefore follows that upon activation an additional enzyme structural change occurs or a new protein−lipid complex is formed. This new form is characterized by its high affinity for calcium and its increased catalytic ability. It should be noted that formation of this highly active form occurs simultaneously with or just subsequently to large morphological changes in the bilayer promoted by product accumulation.

REFERENCES

1. Renetseder, R., Brunie, S., Dijkstra, B. W., Drenth, J., and Sigler, P. B. (1985) *J. Biol. Chem. 260*, 11627−11634.
2. Maraganore, J. M., and Heinrikson, R. L. (1993) *J. Biol. Chem. 268*, 6064.
3. Maraganore, J. M., and Heinrikson, R. L. (1986) *J. Biol. Chem. 261*, 4797−4804.
4. Verheij, H. M., Slotboom, A. J., and de Haas, G. H. (1981) *Rev. Physiol. Biochem. Pharmacol. 91*, 91−203.
5. Mayer, R. J., and Marshall, L. A. (1993) *FASEB J. 7*, 339−348.
6. Scott, D. L., and Sigler, P. B. (1994) *Adv. Protein Chem. 45*, 53−88.
7. Dennis, E. A. (1994) *J. Biol. Chem. 269*, 13057−13060.
8. Jain, M. K., Ranadive, G., Yu, B. Z., and Verheij, H. M. (1991) *Biochemistry 30*, 7330−7340.
9. Lathrop, B. K., and Biltonen, R. L. (1992) *J. Biol. Chem. 267*, 21425−21431.
10. Bell, J. D., and Biltonen, R. L. (1989) *J. Biol. Chem. 264*, 12194−12200.
11. Lichtenberg, D., Romero, G., Menashe, M., and Biltonen, R. L. (1986) *J. Biol. Chem. 261*, 5334−5340.
12. Honger, T., Jorgensen, K., Biltonen, R. L., and Mouritsen, O. G. (1996) *Biochemistry 35*, 9003−9006.
13. Biltonen, R. L., Heimburg, T. R., Lathrop, B. K., and Bell, J. D. (1989) *Adv. Exp. Med. Biol. 279*, 85−103.
14. Burack, W. R., Yuan, Q., and Biltonen, R. L. (1993) *Biochemistry 32*, 583−589.
15. Burack, W. R., Dibble, A. R. G., Allietta, M. M., and Biltonen, R. L. (1977) *Biochemistry 36*, 10551−10557.
16. Tatulian, S. A., Biltonen, R. L., and Tamm, L. K. (1997) *J. Mol. Biol. 268*, 809−815.
17. Bell, J. D., and Biltonen, R. L. (1992) *J. Biol. Chem. 267*, 11046−11056.
18. Romero, G., Thompson, K., and Biltonen, R. L. (1987) *J. Biol. Chem. 262*, 13476−13482.
19. Lin, Y., Nielsen, R., Murray, D., Hubbell, W. L., Mailer, C., Robinson, B. H., and Gelb, M. H. (1998) *Science 279*, 1925−1929.
20. Gelb, M. H., Cho, W., and Wilton, D. C. (1999) *Curr. Opin. Struct. Biol. 9*, 428−432.
21. Han, S. K., Yoon, E. T., Scott, D. L., Sigler, P. B., and Cho, W. (1997) *J. Biol. Chem. 272*, 3573−3582.
22. Ghomashchi, F., Lin, Y., Hixon, M. S., Yu, B.-Z., Annand, R., Jain, M. K., and Gelb, M. H. (1998) *Biochemistry 37*, 6697−6710.
23. Sumandea, M., Das, S., Sumandea, C., and Cho, W. (1999) *Biochemistry 38*, 16290−16297.
24. van den Berg, B., Tessari, M., Boelens, R., Dijkman, R., Kaptein, R., de Haas, G. H., and Verheij, H. M. (1995) *J. Biomol. NMR 5*, 110−121.
25. Maliwal, B. P., Yu, B. Z., Szmacinski, H., Squier, T., Binsbergen, J., Slotboom, A. J., and Jain, M. K. (1994) *Biochemistry 33*, 4509−4516.
26. Jerala, R., Almeida, P. F. F., Ye, Q., Biltonen, R. L., and Rule, G. S. (1996) *J. Biomol. NMR 7*, 107−120.

27. Maraganore, J. M., Merutka, G., Cho, W., Welches, W., Kezdy, F. J., and Heinrickson, R. L. (1984) *J. Biol. Chem. 259*, 13839−13843.
28. Lathrop, B., Burack, W. R., Biltonen, R. L., and Rule, G. S. (1992) *Protein Expression Purif. 3*, 512−517.
29. Yanisch-Perron, C., Vieira, J., and Messing, J. (1985) *Gene 33*, 103−119.
30. Kunkel, T. A., Bebenek, K., and McClary, J. (1991) *Methods Enzymol. 204*, 125−139.
31. Sanger, F., Nicklen, S., and Coulson, A. R. (1977) *Proc. Natl. Acad. Sci. U.S.A. 74*, 5463−5467.
32. Yu, B.-Z., Berg, O. G., and Jain, M. K. (1999) *Biochemistry 38*, 10449−10456.
33. Scott, D. L., White, S. P., Otwinowski, Z., Yuan, W., Gelb, M. H., and Sigler, P. B. (1990) *Science 250*, 1541−1546.
34. Yu, B.-Z., Janssen, M. J. W., Verheij, H. M., and Jain, M. K. (2000) *Biochemistry 39*, 5702−5711.
35. Scott, D. L., and Sigler, P. B. (1994) *Adv. Inorg. Biochem. 10*, 139−155.
36. Kuipers, O. P., Vincent, M., Brochon, J. C., Verheij, H. M., Hass, G. H., and Gallay, J. (1991) *Biochemistry 30*, 8771−8785.
37. Peersen, O. B., Pratt, E. A., Truong, H. T. N., Ho, C., and Rule, G. S. (1990) *Biochemistry 29*, 3256−3262.
38. Ludescher, R. D., Johnson, I. D., Volwerk, J. J., de Haas, G. H., Jost, P. C., and Hudson, B. S. (1988) *Biochemistry 27*, 6618−6628.
39. Kuipers, O. P., Kerver, J., van Meersbergen, J., Vis, R., Dijkman, R., Verhij, H. M., and de Haas, G. H. (1990) *Protein Eng. 3*, 599−603.
40. Lee, B. I., Yoon, E. T., and Cho, W. (1996) *Biochemistry 35*, 4231−4240.
41. Dua, R., Wu, S. K., and Cho, W. (1995) *J. Biol. Chem. 270*, 263−268.
42. Jain, M. K., Yu, B. Z., Rogers, J., Ranadive, G. N., and Berg, O. G. (1991) *Biochemistry 30*, 7306−7317.

BI001901N